References and Notes

(1) P. J. Flory, "Statistical Mechanics of Chain Molecules", Wiley, New York, N.Y., 1969.
(2) P. J. Flory, *Macromolecules*, **7**, 381 (1974).
(3) W. L. Mattice, *Macromolecules*, **8**, 644 (1975).
(4) W. L. Mattice, *Macromolecules*, **9**, 48 (1976); **10**, 1177 (1977).
(5) W. L. Mattice, *Macromolecules*, **10**, 511, 516 (1977); **11**, 15 (1978).
(6) A. Abe, *Polym. J.*, **1**, 232 (1970); *J. Polym. Sci., Polym. Symp.*, **54**, 135 (1976); *Macromolecules*, **10**, 34 (1977).
(7) W. L. Mattice, *Macromolecules*, **10**, 1171 (1977).
(8) V. Crescenzi and P. J. Flory, *J. Am. Chem. Soc.*, **86**, 142 (1964).
(9) C.-L. Lee and F. A. Emerson, *J. Polym. Sci., Part A-2*, **5**, 829 (1967).
(10) J. E. Mark, D. S. Chiu, and T.-K. Su, *Polymer*, in press.
(11) P. J. Flory, V. Crescenzi, and J. E. Mark, *J. Am. Chem. Soc.*, **86**, 146 (1964).
(12) J. E. Mark, *J. Chem. Phys.*, **49**, 1398 (1968).
(13) A. Abe, R. L. Jernigan, and P. J. Flory, *J. Am. Chem. Soc.*, **88**, 631 (1966).
(14) P. J. Flory and J. E. Mark, *Makromol. Chem.*, **75**, 11 (1964).
(15) R. R. Rahalkar, D. S. Chiu, and J. E. Mark, personal communication.
(16) J. E. Mark and P. J. Flory, *J. Am. Chem. Soc.*, **86**, 138 (1964).

Rheooptical Studies on the Deformation Mechanism of Polymer Spherulite by Linear Elastic Theory[1a]

Masaru Matsuo,*[1b] Tetsuya Ogita,[1b] Shoji Suehiro,[1c] Takeshi Yamada,[1c] and Hiromichi Kawai[1c]

Department of Textile Engineering, Faculty of Engineering, Yamagata University, Yonezawa 992, Japan, and Department of Polymer Chemistry, Faculty of Engineering, Kyoto University, Kyoto 606, Japan.

Received February 22, 1977

ABSTRACT: A mathematical representation for the deformation mechanism of polymer spherulites is proposed in terms of the relationship between optical and mechanical responses to external mechanical excitations by using a linear elastic theory. The optical quantities observed from x-ray diffraction and polarized light scattering are found to be a sort of average of mechanical quantities, such as strains and stresses arising locally in the spherulites. In addition, the theoretical treatment is also tested with experimental results. Both the experimental results with regard to lattice deformations of crystalline regions and light scattering are found to be rather close to the calculated ones.

I. Introduction

The broad aim of this paper is to construct a theory for rheooptical studies that have revealed characteristic relaxation times of the responses of structural units in polymer solids to external mechanical excitations. The experimental results have been discussed in a number of papers.[2-7] The recent results of rheooptical investigations, using the dynamic x-ray diffraction technique[8,9] for dynamic orientation and lattice deformation of polyethylene crystal[10-12] as well as the dynamic light-scattering technique[13,14] for the deformation mechanism of polyethylene spherulites,[15,16] are the most definitive evidence confirming the notion that the α mechanical dispersion of polyethylene is actually related to the crystalline responses. However, the relationship between optical and mechanical responses to external mechanical excitation has never been developed in mathematical and quantitative terms. Quantitative description of the viscoelastic behavior of crystalline polymers in bulk is a very complicated and difficult problem, reflecting their complex structures.

The first investigation of the mathematical description of elastic behavior of a spherically isotropic system under general loading was carried out by Chen,[17] and its mathematical procedure was applied to the deformation mechanism of polyethylene spherulites by Wang.[18,19] Hence, this paper is concerned with a mathematical description of the relationship between the optical and mechanical responses using linear elastic theory. The investigation is mainly carried out for the problem in the deformation of polyethylene having a spherulitic crystalline texture in order to discuss the crystal lattice deformation within the spherulite and the polarized light scattering from the spherulitic texture in a quantitative manner. This treatment may not be sufficient, as discussed above, and therefore a more quantitative treatment supplementing the viscoelastic properties of the materials will be discussed in the succeeding paper.[20]

First, the five elastic constants C_{ij} for the spherically isotropic material will be determined by using an aggregation model proposed by Hibi,[21] and the mechanical constants in bulk, shear modulus G, bulk modulus K, Young's modulus E, and Poisson's ratio ν will be calculated by the method of Wang.[18]

Second, a mathematical representation of the crystal lattice strains within the spherulite will be discussed in terms of the geometric arrangement of the bulk specimen as revealed by x-ray optical coordinates. The calculated results will be tested vs. results obtained from dynamic x-ray diffraction measurements of a low density polyethylene (Sumikathen G201) and a high-density polyethylene (Sholex 5065).[22]

Finally, the light scattering from the spherulite will be calculated from a knowledge of the principal polarizability distribution within the spherulite, omitting the molecular orientation of the medium around the spherulite.

II. Elastic Constants of Polyethylene Lamella and in Bulk

Hooke's law in a polyethylene spherulite may be written by using a special spherical coordinate system suggested by Chen[17] and Wang[18] as follows:

$$\sigma_{\theta\theta} = C_{11}\epsilon_{\theta\theta} + C_{12}\epsilon_{\phi\phi} + C_{13}\epsilon_{rr}$$
$$\sigma_{\phi\phi} = C_{12}\epsilon_{\theta\theta} + C_{11}\epsilon_{\phi\phi} + C_{13}\epsilon_{rr}$$
$$\sigma_{rr} = C_{13}(\epsilon_{\theta\theta} + \epsilon_{\phi\phi}) + C_{33}\epsilon_{rr}$$
$$\sigma_{r\theta} = C_{44}\epsilon_{r\theta}$$
$$\sigma_{r\phi} = C_{44}\epsilon_{r\phi}$$
$$\sigma_{\theta\phi} = \tfrac{1}{2}(C_{11} - C_{12})\epsilon_{\theta\phi} \quad (1)$$

where the symbols σ_{ij}, ϵ_{ij}, and C_{ij} denote components of stress, strain, and elastic stiffness, respectively. The subscript 3 of

0024-9297/78/2211-0521$01.00/0

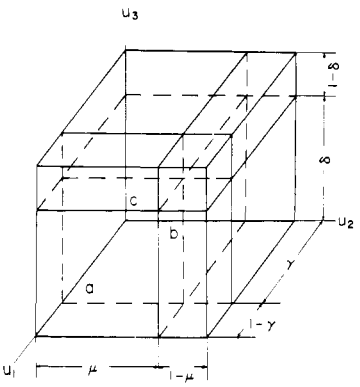

Figure 1. Composite structural unit of a semicrystalline polymer with an orthorhombic crystalline surrounded by an amorphous phase.

σ_{ij}, ϵ_{ij}, and C_{ij} is chosen in the radial direction. For example, C_{33} is the stiffness in the radial direction. The five elastic stiffnesses are very significant in constructing the rheooptical theory as well as mechanical properties of crystalline polymers and are known to be strongly dependent on the manner in which crystals and amorphous fractions are organized. Several models have been proposed.[23-25] Wang[25] studied the anisotropic elastic properties of transcrystalline polyethylene composed of aligned narrow spherulites (which is the so-called cylindrical spherulite) by employing the composite theories of Hill,[26] Hermans,[27] and Kroner[28] to account for mechanical interactions between the two phases and between the individual spherulites. The procedure was extended to bulk linear polyethylene with a spherulitic texture.

In this paper, a model for the composite structural unit proposed by Hibi et al.[21] is adopted to determine the values of C_{ij} in eq 1 from the standpoint of composite crystals being a little different from the above proposals.[23-28] The values may be obtained from those of the elastic stiffness of composite structural units comprising crystal lamella and amorphous phase.

Let the composite structural unit be modeled as shown in Figure 1, in which an isotropic noncrystalline layer lies adjacent to an orthorhombic crystal with the interface perpendicular to the U_3, U_2, and U_1 axes, so that the crystallinity of polyethylene spherulite is represented by $\delta \times \gamma \times \mu$. The U_3, U_2, and U_1 axes correspond to the crystal c, b, and a axes, respectively. We may here define the elastic stiffnesses of the composite structural unit in Figure 1 as C_{ij}^{w}.

The C_{ij} are related to C_{ij}^{w} via the orientation of crystal lamella within the spherulite. Actually, the lamellae are composed of minute crystals whose b axes are oriented in the radial direction, while the c and a axes are in the tangential direction and rotate about the radius in a helicoidal manner. Hence, the relation may be given by

$$C_{11} = \tfrac{1}{8}(3C_{11}^{w} + 3C_{33}^{w} + 2C_{13}^{w} + 4C_{55}^{w})$$
$$C_{22} = C_{11}$$
$$C_{33} = C_{22}^{w}$$
$$C_{12} = \tfrac{1}{8}(C_{11}^{w} + C_{33}^{w} + 6C_{13}^{w} - 4C_{55}^{w})$$
$$C_{13} = \tfrac{1}{2}(C_{12}^{w} + C_{23}^{w})$$
$$C_{23} = C_{13}$$
$$C_{44} = \tfrac{1}{2}(C_{44}^{w} + C_{66}^{w})$$
$$C_{55} = C_{44}$$
$$C_{66} = \tfrac{1}{8}(C_{11}^{w} + C_{33}^{w} - 2C_{13}^{w} + 4C_{55}^{w}) \quad (2)$$

The subscript 3 of the elastic stiffnesses C_{ij} in eq 1 (or eq 2) is chosen in the radial direction, while the subscript 3 of the elastic stiffnesses C_{ij}^{w} is chosen in the direction of the U_3 axis, the subscript 2 in the direction of the U_2 axis, and the subscript 1 in the direction of the U_1 axis, respectively. The elastic stiffnesses C_{ij}^{w} may be related to the elastic compliances S_{ij}^{w} as follows:

$$C_{ij}^{w} = (-1)^{i+j}\Delta_{ij}^{s}/\Delta^{s} \quad (3)$$

$$\Delta^{s} = \begin{vmatrix} S_{11}^{w} & S_{12}^{w} & S_{13}^{w} & 0 & 0 & 0 \\ S_{12}^{w} & S_{22}^{w} & S_{23}^{w} & 0 & 0 & 0 \\ S_{13}^{w} & S_{23}^{w} & S_{33}^{w} & 0 & 0 & 0 \\ 0 & 0 & 0 & S_{44}^{w} & 0 & 0 \\ 0 & 0 & 0 & 0 & S_{55}^{w} & 0 \\ 0 & 0 & 0 & 0 & 0 & S_{66}^{w} \end{vmatrix} \quad (4)$$

where Δ_{ij}^{s} is the determinant of the matrix obtained by omitting the ith line and the jth rank in the matrix S_{ij}^{w} and Δ^{s} is the determinant of matrix S_{ij}^{w}. The elastic compliances S_{ij}^{w} can be calculated on the basis of a homogeneous stress hypothesis by using the elastic compliance of the crystallite S_{ij}^{co} and the elastic compliance of the amorphous phase S_{ij}^{ao}. The calculating methods have been described in detail by Hibi et al. elsewhere.[21] The values of elastic compliances S_{ij}^{co} of the polyethylene crystal unit can be determined from the inverse matrix of the elastic stiffnesses C_{ij}^{co} of the unit proposed by Odajima et al.,[30] while the values of elastic compliances S_{ij}^{ao} of the amorphous phase are quite uncertain. Recent observation of intercrystalline link and tie molecules in crystalline polymers[31] suggests that the amorphous phase might be locally anisotropic. However, the present knowledge of the amorphous structure is not quantitative enough to permit a good estimate of the anisotropic moduli of the amorphous phase,[31,32] and we shall assume the amorphous structure to be isotropic and hence characterizable by two independent elastic constants. Actually, the two elastic compliances may be approximated as $S_{11}^{ao} = 5.1 \times 10^{-10}$ and $S_{12}^{ao} = -2.5 \times 10^{-10}$ cm^2/dyn on the basis of the amorphous phase of polyethylene being in a rubbery state over a range of temperature from room temperature up to around 80 °C.

Figure 2 shows the results of calculation of the stiffnesses C_{ij} in the spherulite as a function of crystallinity X_c by using the model in Figure 1 and assuming that $\delta = \gamma = \mu$. As illustrated in Figure 2, C_{11}, C_{66}, and C_{12} increase rapidly with increase of crystallinity, while C_{33}, C_{13}, and C_{44} are hardly affected by the crystallinity. The X_c dependences of the elastic stiffnesses in Figure 2 are similar to those obtained by Wang.[25]

Figure 3 shows the X_c dependences of mechanical constants in bulk, that is, bulk modulus K, shear modulus G, Young's modulus E, and Poisson's ratio ν, calculated from the values of the five stiffnesses illustrated in Figure 2 by using the procedure suggested by Wang.[18] The dependences in Figure 3 are nearly the same as those of Wang, and these results at the appropriate degree of crystallinity agree fairly well with the experimental results for Young's modulus and the shear modulus of polyethylene reported by McCrum and Morris.[33]

III. Crystal Strains in a Spherulite Detected by X-ray Diffraction

A. Mathematical Representation of Crystal Strains in a Spherulite. A mathematical representation of crystal strains in the spherulite will be discussed in terms of a geometrical arrangement of the test specimen against x-ray optical coordinate. To understand the mechanism leading to crystal strains within the spherulite, it is important to distinguish two strain quantities: one arising locally in the

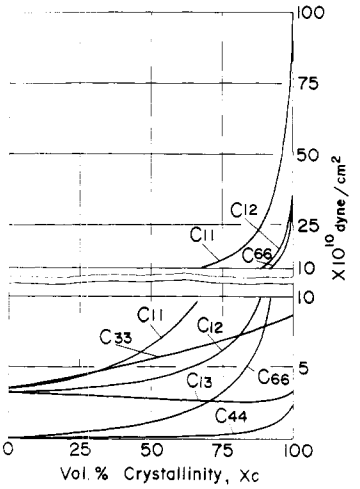

Figure 2. Elastic constants in a polyethylene spherulite.

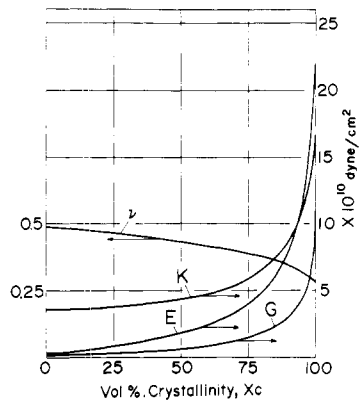

Figure 3. Distribution functions of mechanical constants in bulk to crystallinity.

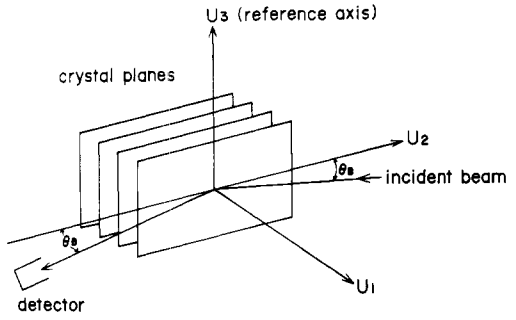

Figure 4. Geometrical arrangement of crystal planes against x-ray optical coordinate O-$U_1U_2U_3$.

spherulite and the other detected by x-ray diffraction measurements. Hence, we present now a conclusion that the latter may be a sort of average of the former and may be related to the former through a somewhat complicated mathematical relationship.

Figure 4 shows the geometrical relation of the crystal plane to the x-ray optical coordinate. The U_1 axis may be taken along the reciprocal lattice vector of the crystal plane and the U_3 axis along the reference axis. The U_2 axis is perpendicular to the U_1U_3 plane. For a Cartesian coordinate O-$V_1V_2V_3$ within a lamella, the V_3, V_2, and V_1 axes are taken along the direction of strains ϵ_{rr}, $\epsilon_{\theta\theta}$, and $\epsilon_{\phi\phi}$, respectively. The Cartesian coordinate O-$V_1V_2V_3$ may be specified by using two Euler angles ϕ and θ with respect to a space of film specimen O-

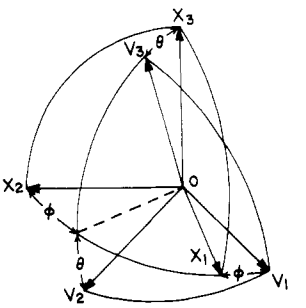

Figure 5. Eular angles θ and ϕ, which specify the orientation of Cartesian coordinate O-$V_1V_2V_3$ fixed in a lamella with respect to another Cartesian coordinate O-$X_1X_2X_3$ fixed in the bulk specimen.

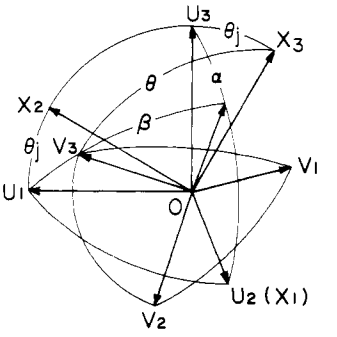

Figure 6. Coordinate system for crystal strain detected by x-ray diffraction technique against bulk specimen coordinate.

$X_1X_2X_3$ as shown in Figure 5. The V_3 axis may be specified by using two Euler angles β and α with respect to the optical coordinate O-$U_1U_2U_3$ as shown in Figure 6. The Cartesian coordinate O-$X_1X_2X_3$ is fixed within the film specimen, so that the X_3 axis takes along the direction of external excitation, the X_1 axis the direction of film thickness, and the X_2X_3 plane is parallel to the film surface. The angle θ_j is the polar angle between the U_3 axis and the X_3 axis. The distribution of the jth crystal lattice strain may be observed as the function of the polar angle θ_j by the rotation of the X_3 axis around the X_1 axis.

From the angular relation as shown in Figures 5 and 6, one may obtain the following three equations.

$$(\mathbf{V}_3 \cdot \mathbf{U}_1) = -\cos\theta \sin\theta_j + \sin\theta \cos\phi \cos\theta_j \quad (5)$$

$$(\mathbf{V}_2 \cdot \mathbf{U}_1) = \sin\theta \sin\theta_j + \cos\theta \cos\phi \cos\theta_j \quad (6)$$

$$(\mathbf{V}_1 \cdot \mathbf{U}_1) = -\sin\phi \cos\theta_j \quad (7)$$

On the other hand, the strain $\epsilon_{U_{1j}}$ in the U_1 direction which reveals the strain in the direction of the reciprocal lattice vector of the jth crystal plane may be given by using the strains ϵ_{rr}, $\epsilon_{\theta\theta}$, $\epsilon_{\phi\phi}$, and $\epsilon_{r\theta}$ in the spherulite.

$$\epsilon_{U_{1j}} = (\mathbf{V}_3 \cdot \mathbf{U}_1)^2\epsilon_{rr} + (\mathbf{V}_2 \cdot \mathbf{U}_1)^2\epsilon_{\theta\theta} + (\mathbf{V}_1 \cdot \mathbf{U}_1)^2\epsilon_{\phi\phi} + (\mathbf{V}_3 \cdot \mathbf{U}_1)(\mathbf{V}_2 \cdot \mathbf{U}_1)\epsilon_{r\theta} \quad (8)$$

Considering the geometrical arrangement concerning the orientation of crystal units in the polyethylene spherulite against the x-ray optical coordinate, the crystallites in the spherulite detected by the x-ray diffraction measurements are found to be situated only on the area of the cone which is formed by the rotation of the V_3 axis around the U_1 axis in Figure 6. Hence, the strain quantity $\Delta\epsilon_{U_{1j}}$ observed from the x-ray diffraction may be given by

$$\Delta\epsilon_{U_{1j}} = \frac{1}{\pi a^2 \sin\beta \cos\beta} \int_0^{2\pi} \int_0^{a} \epsilon_{U_{1j}} r \sin\beta \cos\beta \, dr \, d\alpha \quad (9a)$$

$$\Delta\epsilon_{U_{1j}} = \frac{1}{\pi a^2}\int_0^{2\pi}\int_0^a \epsilon_{U_{1j}} r\, dr\, d\alpha \tag{9b}$$

The angle β in eq 9a may be related as follows:

$$\sin\beta = \sin\Theta_j \sin\Phi_j \tag{10}$$

The angles Θ_j and Φ_j are polar and azimuthal angles specifying the orientation of the reciprocal lattice vector of the jth crystal plane with respect to an orthorhombic crystal unit.

Moreover, one may obtain the following three equations from the angular relation obtained as shown in Figures 4 through 6.

$$\cos\theta = \cos\beta\cos\alpha\cos\theta_j - \sin\beta\sin\theta_j \tag{11}$$

$$\sin\theta\sin\phi = \cos\beta\sin\alpha \tag{12}$$

$$\sin\theta\cos\phi = \sin\beta\cos\theta_j + \cos\beta\cos\alpha\sin\theta_j \tag{13}$$

By using the linear elastic theory, the strains of the spherulite are given by Wang.[19]

$$\epsilon_{rr} = A_{01}K_{01}(\nu_{01} - 1/2)r^{\nu_{01}-3/2} + \frac{(3\cos^2\theta - 1)}{2} \times \sum_{i=1,3} A_{2i}K_{2i}(\nu_{2i} - 1/2)r^{\nu_{2i}-3/2} \tag{14}$$

$$\epsilon_{\theta\theta} = A_{01}K_{01}r^{\nu_{01}-3/2} + 1/2\sum_{i=1,3} A_{2i}\{3(K_{2i} - 4)\cos^2\theta - K_{2i} + 6\}r^{\nu_{2i}-3/2} \tag{15}$$

$$\epsilon_{\phi\phi} = A_{01}K_{01}r^{\nu_{01}-3/2} + 1/2\sum_{i=1,3} A_{2i}\{3(K_{2i} - 2)\cos^2\theta - K_{2i}\}r^{\nu_{2i}-3/2} \tag{16}$$

$$\epsilon_{r\theta} = -3\sin\theta\cos\theta\sum_{i=1,3} A_{2i}(K_{2i} + \nu_{2i} - 3/2)r^{\nu_{2i}-3/2} \tag{17}$$

$$\epsilon_{r\phi} = \epsilon_{\theta\phi} = 0 \tag{18}$$

where the coefficients A_{ni} are arbitrary constants to be determined from boundary conditions, and the coefficients ν_{ni} and K_{ni} are also constants calculated by Chen.[17]

According to eq 5 through 18, eq 9b may be finally given by the function of polar angle θ_j.

$$\Delta\epsilon_{U_{1j}}(\theta_j) = \frac{2A_{01}K_{01}}{(\nu_{01} + 1/2)}\{(\nu_{01} - 3/2)\sin^2\Theta_j\sin^2\Phi_j + 1\}a^{\nu_{01}-3/2} + 1/2(3\cos^2\theta_j - 2)\sum_{i=1,3}\frac{A_{2i}}{(\nu_{2i} + 1/2)} \times [3(K_{2i} - 2)(1 - \sin^2\Theta_j\sin^2\Phi_j)\{(\nu_{2i} - 5/2) - (\nu_{2i} - 7/2) \times (1 - \sin^2\Theta_j\sin^2\Phi_j)\} - 2K_{2i}]a^{\nu_{2i}-3/2} \tag{19}$$

Considering the unit cell dimensions of polyethylene, the strains in the normal direction of the (110), (200), and (020) crystal planes may be obtained by using ($\Theta_j = \pi/2$, Φ_j = 7.49/4.94), ($\Theta_j = \pi/2$, $\Phi_j = 0$), and ($\Theta_j = \pi/2$, $\Phi_j = \pi/2$), respectively.

If the crystal unit is completely isotropic, the following relations can be obtained, as suggested by Chen[17] and Wang;[18,19]

$$\nu_{01} = 3/2, \quad \nu_{21} = 7/2, \quad \nu_{23} = 3/2, \quad K_{23} = 2, \quad A_{21} = 0 \tag{20}$$

Substituting eq 20 into eq 19, the following relation may be obtained

$$\Delta\epsilon_{U_{1j}}(\theta_j) = A_{01}K_{01} - A_{23}(3\cos^2\theta_j - 2) \tag{21}$$

From the above result, one can understand that the strain distribution for the completely isotropic crystal unit is independent of different kinds of crystal planes. Equation 19 reveals the theoretical distribution of the strain of the jth crystal plane corresponding to the experimental distribution observed from the x-ray diffraction technique only at 100% crystallinity. In the semicrystalline case, it reveals the distribution of the total strain of the jth crystal plane and the amorphous phase in the U_1 direction.

B. Test Specimens and Experimental Procedure. As discussed already, a high-density polyethylene, Sholex 5065, and a low-density polyethylene, Sumikathene G201, were used as test specimens. The pellets of the high-density polyethylene were melted at 170 °C in a laboratory press under a pressure of 200 kg/cm^2 and slowly cooled down to room temperature. The volume percent crystallinity which was measured by the ethanol–water density gradient tube method was found to be 74%. On the other hand, the pellets of the low-density polyethylene were melted at 140 °C and slowly cooled down to 105 °C, then the specimens were quenched by being plunged into an ice–water bath and further annealed at 130 °C for 2 h. The volume percent crystallinity was found to be 46%.

The dynamic x-ray diffraction intensity distribution was measured by using a narrow sector technique[34] along the equatorial and meridional directions. The measurements were made at the maximum and minimum strain phases for a relatively narrow interval of ±10° over a frequency range from 0.2 to 3.2 Hz at four different temperatures 30, 60, 70, and 86.5 °C. As mentioned briefly in the introduction, the theoretical results were calculated on the basis of a linear elastic theory which neglects the viscoelastic contributions from the polymer spherulite. In order to compare analytical results with the data obtained from dynamic x-ray measurements, the theoretical elastic crystal lattice strain is assumed to be equivalent to the in-phase component of the measured dynamic strain[9,10] of the jth crystal plane. This is because of the difficulty of observing the crystal strain in the static state.

C. Experimental Results and Discussion. By using the stress $\Delta\sigma_{U_{1j}}(\theta_j)$ associated with $\Delta\epsilon_{U_{1j}}(\theta_j)$ on the basis of the homogeneous stress hypothesis, the strain $\Delta\epsilon_c(\theta_j)$ of the jth crystal plane and $\Delta\epsilon_{U_{1j}}(\theta_j)$ on the area of cone discussed already in eq 9b may be given by

$$\Delta\epsilon_c(\theta_j) = S_{cj}\Delta\sigma_{U_{1j}}(\theta_j) \tag{22}$$

and

$$\Delta\epsilon_{U_{1j}}(\theta_j) = S_{tj}\Delta\sigma_{U_{1j}}(\theta_j) \tag{23}$$

where S_{cj} is the compliance of the jth crystal plane and S_{tj} is the average compliance of the jth crystal plane and the amorphous phase. Accordingly, we have

$$\Delta\epsilon_c(\theta_j)/\Delta\epsilon_{U_{1j}}(\theta_j) = S_{cj}/S_{tj} \tag{24}$$

Thus, at $\theta_j = 90°$,

$$\Delta\epsilon_c(90)/\Delta\epsilon_{U_{1j}}(90) = S_{cj}/S_{tj} \tag{25}$$

so that from eq 24 and 25,

$$\Delta\epsilon_{U_{1j}}(\theta_j)/\Delta\epsilon_{U_{1j}}(90) = \Delta\epsilon_c(\theta_j)/\Delta\epsilon_c(90) \tag{26}$$

Equation 26 indicates that the distribution of the total strain normalized with the strain at polar angle $\theta_j = 90°$ is equivalent to that of crystal strain normalized with the strain at the same angle. This normalized relationship should allow a better comparison between the calculated results and the experimental data.

Figure 7 shows the calculated and observed distributions using the normalized quantities where $\Delta\epsilon_{\theta j}$ and $\Delta\epsilon_{90°}$ are abbreviations of $\Delta\epsilon_c(\theta_j)$ and $\Delta\epsilon_c(90)$, respectively. It can be seen that irrespective of the crystallinity level, temperature, and frequency, a fairly good agreement between the calculated and the observed results can be achieved after the normalization. Thus, the normalization procedure renders the results independent of the intrinsic properties of polymer crystals such

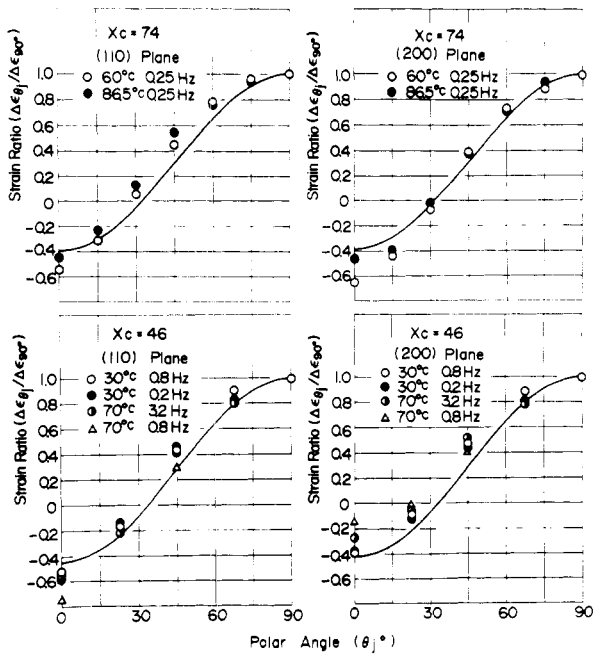

Figure 7. Strain distributions of the (110) and (200) crystal planes observed from the x-ray diffraction technique with those calculated (solid curves). Both distributions are normalized at a polar angle $\theta_j = 90°$.

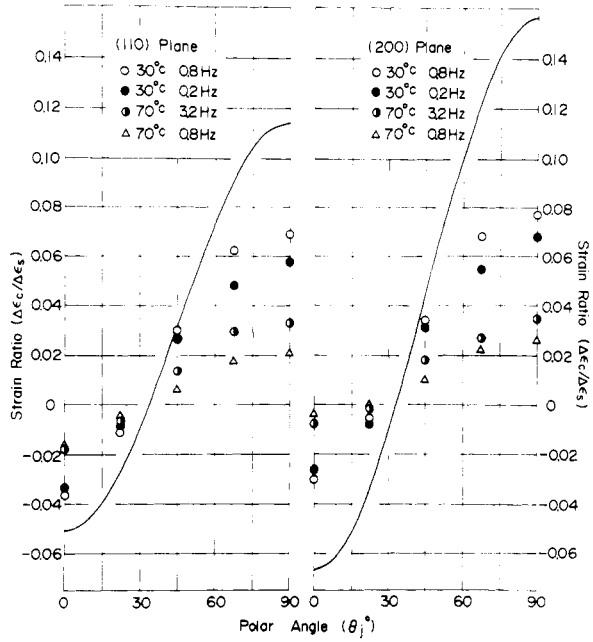

Figure 8. Strain distributions of the (110) and (200) crystal planes observed from the x-ray diffraction technique with those calculated (solid curves).

as temperature and frequency and facilitates comparison between theory and experiment.

The comparison illustrated in Figure 7 is not necessarily rigorous since we may also compare the calculated results with the experimental ones by normalizing them in terms of the bulk strain.

On the basis of eq 22 and 23, the theoretical strain of the jth crystal plane has been calculated as follows:

$$\Delta\epsilon_c(\theta_j) = \frac{S_{cj}}{S_{tj}} \Delta\epsilon_{U_{1j}}(\theta_j) \tag{27}$$

where

$$S_{tj} = S_{11}\cos^4\Phi_j + S_{33}\sin^4\Phi_j + \sin^2\Phi_j\cos^2\Phi_j(2S_{13} + S_{44}) \tag{28a}$$

$$S_{cj} = S_{11}^c\cos^4\Phi_j + S_{33}^c\sin^4\Phi_j + \sin^2\Phi_j\cos^2\Phi_j(2S_{13}^c + S_{44}^c) \tag{28b}$$

where

$$S_{11} = \tfrac{1}{8}(3S_{11}^w + 3S_{33}^w + 2S_{13}^w + S_{55}^w)$$
$$S_{33} = S_{22}^w$$
$$S_{13} = \tfrac{1}{2}(S_{12}^w + S_{23}^w)$$
$$S_{44} = \tfrac{1}{2}(S_{44}^w + S_{66}^w)$$
$$S_{11}^c = \tfrac{1}{8}(3S_{11}^{co} + 3S_{33}^{co} + 2S_{13}^{co} + S_{55}^{co})$$
$$S_{33}^c = S_{22}^{co}$$
$$S_{13}^c = \tfrac{1}{2}(S_{12}^{co} + S_{23}^{co})$$
$$S_{44}^c = \tfrac{1}{2}(S_{44}^{co} + S_{66}^{co}) \tag{29}$$

where S_{ij} are compliances at 46% crystallinity and S_{ij}^c are the compliances at 100% crystallinity.

Figure 8 shows the calculated and experimental results, in which $\Delta\epsilon_c$ is an abbreviation of $\Delta\epsilon_c(\theta_j)$ in eq 27. As can be seen in Figure 8, the experimental results depend on temperature and frequency but exhibit a similar dependence in both (110) and (200) crystal planes. By contrast, the calculated distribution is sharper for the (200) crystal plane than for the (110) crystal plane, and further, in both cases, they deviate appreciably from the observed ones even at room temperature. Although this would suggest that the comparison should be made in the static state at room temperature, it is very difficult to measure the crystal strain in the static state because of the viscoelastic nature of the material.

IV. Light Scattering

A. Procedure for Calculation. The light scattering from deformed two-[35] and three-dimensional[36] spherulites has been studied by Stein et al. In their calculations for the deformed three-dimensional spherulite, two types of density distributions of scattering elements within the deformed spherulite were assumed in addition to the affine deformation. In this paper, the light-scattering pattern will be analyzed using a different approach, namely, it will be calculated from the knowledge of the principal polarizability distribution in the spherulite on the assumptions that, (1) there exists a stress optical coefficient which is constant throughout the spherulite and, (2) molecular orientation of the medium around the spherulite is random.

For a system having three different principal stresses P_i, three different refractive indexes n_i may be calculated by using the relation

$$n_i - n_j = C(P_i - P_j) \tag{30}$$

where C is the stress–optical coefficient.

The three different principal stresses, as suggested by Stein et al.,[37] may be obtained as

$$P_1 = \sigma_{rr}\cos^2\Delta\theta + 2\sigma_{r\theta}\sin\Delta\theta\cos\Delta\theta + \sigma_{\theta\theta}\sin^2\Delta\theta \tag{31}$$

$$P_2 = \sigma_{rr}\sin^2\Delta\theta - 2\sigma_{r\theta}\sin\Delta\theta\cos\Delta\theta + \sigma_{\theta\theta}\cos^2\Delta\theta \tag{32}$$

$$P_3 = \sigma_{\phi\phi} \tag{33}$$

where

$$\tan 2\Delta\theta = 2\sigma_{r\theta}/(\sigma_{rr} - \sigma_{\theta\theta}) \tag{34}$$

In the Rayleigh–Gans approximation, the light-scattering amplitude E of an anisotropic system is given by

$$E = C' \int_v (\mathbf{M} \cdot \mathbf{O}) \exp\{ik(\mathbf{r} \cdot \mathbf{s})\}\, d\mathbf{r} \quad (35)$$

where **M** is the induced dipole moment in the scattering element d**r** located at **r**; **O** is the unit vector perpendicular to the scattering ray and in the plane of polarization of the light transmitted by the analyzer; $k = 2\pi/\lambda$ where λ is the wavelength of the radiation in the spherulite; and **s** is the propagation vector given by $(\mathbf{s}_0 - \mathbf{s}_1)$ where $\mathbf{s}_0$ and $\mathbf{s}_1$ are the unit vectors of incident and scattered rays.

If one uses the same procedure as suggested by Stein et al.,[37] then

$$\begin{aligned} E_{Hv} = {} & (9/2\pi)CC' \frac{\bar{n}}{V(\bar{n}^2+2)^2} \\ & \times \int_{\epsilon}^{2\pi+\epsilon} \int_0^{\pi} \int_0^{a} [\{2C_{13} - C_{11} - C_{12} \\ & + (C_{33} - C_{13})(\nu_{01} - 1/2)A_{01}K_{01}r^{\nu_{01}+1/2} \\ & + 3/2 \sum_{i=1,3} (C_{13} - C_{11})(K_{2i} - 4) + (C_{13} - C_{12})(K_{2i} - 2) \\ & + (C_{33} - C_{13})(\nu_{2i} - 1/2)K_{2i} - 4C_{44}(K_{2i} \\ & + \nu_{2i} - 3/2)\}A_{2i} \cos^2\theta r^{\nu_{2i}+1/2} - 1/2\{(C_{13} - C_{11})(K_{2i} - 6) \\ & + (C_{33} - C_{13})(\nu_{2i} - 1/2)K_{2i} \\ & + (C_{13} - C_{11})K_{2i} - 6C_{44}(K_{2i} + \nu_{2i} - 3/2)\}A_{2i}r^{\nu_{2i}+1/2}] \\ & \times \cos\epsilon \sin\xi \sin\theta \cos\theta F(\theta',\mu') \sin\theta\, dr\, d\theta\, d\xi \end{aligned} \quad (36)$$

where

$$\tan\epsilon = \tan(\theta'/2)/\sin\mu' \quad (37)$$

$$\xi = \phi - \epsilon \quad (38)$$

and $\bar{n}$ is an average refractive index and V and a are the volume and the radius of the spherulite, respectively.

The scattering function $F(\theta',\mu')$ is given by[38]

$$\begin{aligned} F(\theta',\mu') = \cos[k(\mathbf{r} \cdot \mathbf{s})] = 1 + \sum_{l=1}^{\infty} \frac{(-1)^l}{(2l)!} \left(\frac{4\pi}{\lambda} \sin\frac{\theta'}{2}\right)^{2l} \mathbf{r}^{2l} \\ \times \left[\sum_{j=1}^{l} \binom{2l}{2j-1} (\cos\delta \sin\xi \sin\theta)^{2l-2j+1} (\sin\delta \cos\theta)^{2j-1} \right. \\ \left. + \sum_{j=1}^{l+1} \binom{2l}{2j-2} (\cos\delta \sin\xi \sin\theta)^{2l-2j+2} \right. \\ \left. \times (\sin\delta \cos\theta)^{2j-2}\right] \end{aligned} \quad (39)$$

where

$$\sin\delta = \cos(\theta'/2) \cos\mu' \quad (40)$$

and θ' and μ' are the scattering angle and the azimuthal angle, respectively. The scattering intensity is given by the square of eq 36. If the spherulite is isotropic, the following relations are obtained

$$\begin{aligned} & C_{11} = C_{33}, \quad C_{12} = C_{13}, \quad C_{44} = 1/2(C_{11} - C_{12}), \\ & \nu_{01} = 3/2, \quad \nu_{21} = 7/2, \quad \nu_{23} = 3/2, \quad K_{23} = 2, \quad A_{21} = 0 \end{aligned} \quad (41)$$

Substituting eq 41 into eq 36, eq 36 becomes zero. From this result, it may be deduced that the light scattering does not arise from an isotropic spherulite.

B. Discussion. Figure 9 shows the Hv scattering patterns of the spherulite calculated by using the square of eq 36. As illustrated in Figure 9, all of the lobes are extended in the meridional direction and this tendency becomes more pronounced with decrease of the crystallinity. All of the patterns differ considerably from experimental patterns observed generally at relative small extension ratios. This is due to the fact that in the above calculation we have omitted the contribution from deformation of the spherulite. Thus if we take into account the deformed shape of the spherulite, then we may adopt the following equation for the amplitude E;

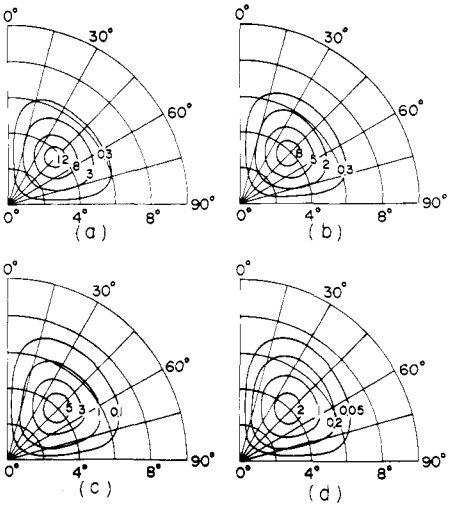

Figure 9. Hv intensity distributions calculated by eq 36 for values of crystallinity, (a) 97%, (b) 74%, (c) 46%, and (d) 12%, in which values of scale 0°, 4°, and 8° mean the degree of scattering angle θ', while values of scale listed in circumference mean the degree of azimuthal angle μ'.

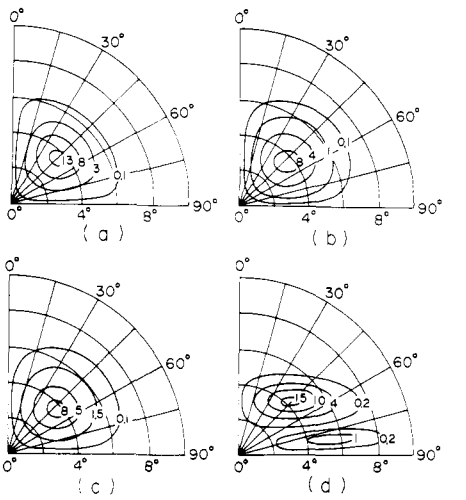

Figure 10. Hv intensity distributions calculated by eq 42 for values of crystallinity, (a) 97%, (b) 74%, (c) 66%, and (d) 46%, in which values of scale 0°, 4°, and 8° mean the degree of scattering angle θ', while values of scale listed in circumference mean the degree of azimuthal angle μ'.

$$\begin{aligned} E = {} & \frac{C'}{V} \int_0^{2\pi} \int_0^{\pi} \int_0^{a+u_a} (\mathbf{M} \cdot \mathbf{O}) \\ & \times \cos[k(\mathbf{r} \cdot \mathbf{s})] r^2 \sin\theta\, dr\, d\theta\, d\phi \\ = {} & -2\pi \frac{C'}{V} \int_0^{\pi} \int_0^{a+u_a} (\mathbf{M} \cdot \mathbf{O}) \\ & \times \sin[2kr \sin(\theta'/2) \cos(\theta'/2) \cos\theta] \\ & \times J_1[2kr \sin(\theta'/2) \cos(\theta'/2) \sin\mu' \sin\theta] r^2 \sin\theta\, dr\, d\theta \end{aligned} \quad (42)$$

where $J_1(x)$ is the first-order Bessel function of x, and u_a is the displacement at the radius a of the spherulite.

The calculation of eq 42 for the present example was carried out numerically and the results for the Hv patterns are shown in Figure 10. It can be seen that at high crystallinities (97, 74, and 66%), the lobes are extended in the equatorial direction which agree fairly well with the experimental results.[39,40] On the other hand, at low crystallinities (46%) the theory predicts

an eight-leaf pattern which has also been observed in a uniaxially stretched low-density polyethylene sample (Yukalon YK-3200) having a rather imperfect texture.[41]

V. Conclusion

This paper was concerned with the relation between mechanical and optical quantities. The strain distribution in the spherulite was transformed into the strains in the crystallites for comparison with the x-ray diffraction measurements. Fairly good agreement between the calculated and experimental results was achieved when the results were normalized with corresponding values at the polar angle $\theta_j = 90°$. Since the results did not reveal detailed information on intrinsic properties of polymer which depend on temperature and frequency, further comparisons were made by normalizing the crystal strain with the bulk strain. In this instance, however, the calculated results did not agree well with the experimental results even at room temperature. This discrepancy might be attributed to the fact that the results calculated from the linear elastic theory were not entirely equivalent to the in-phase component of the dynamic crystal lattice deformation data.

The light-scattering patterns were calculated from the relation between stress and birefringence. In general, the scattering patterns calculated by using eq 42 gave a good agreement with observed ones. Despite the good agreement, however, it is noted that the analysis did not take into account an important factor, namely, the total stress optical coefficient is actually the sum of contributions from the crystalline and amorphous phases for a semicrystalline polymer such as polyethylene.

Acknowledgment. The authors are indebted to Dr. Wang, Bell Laboratories, Murray Hill, N.J., for his valuable comments and suggestions on the manuscripts. Thanks are also due to Dr. Nagaya, Faculty of Engineering, Yamagata University, for his helpful comments.

References and Notes

(1) (a) Presented partly at the 25th Annual Meeting of the Society of Polymer Science, Japan, Tokyo, May 1976; (b) Yamagata University; (c) Kyoto University. To whom correspondence should be addressed.
(2) (a) R. S. Stein, S. Onogi, K. Sasaguri, and D. A. Keedy, *J. Appl. Phys.*, **34,** 80 (1963); (b) R. Yamada, C. Hayashi, S. Onogi, and M. Horio, *J. Polym. Sci., Part C*, **5,** 123 (1964).
(3) S. Onogi and T. Asada, *J. Polym. Sci., Part C*, **16,** 1445 (1967).
(4) S. Onogi, T. Asada, Y. Fukui, and T. Fujisawa, *J. Polym. Sci., Part A-2*, **5,** 1067 (1967).
(5) S. Onogi, T. Asada, and A. Tanaka, *J. Polym. Sci., Part A-2*, **7,** 171 (1969).
(6) Y. Kukui, T. Sato, M. Ushirokawa, T. Asada, and S. Onogi, *J. Polym. Sci., Part A-2*, **8,** 1195 (1970).
(7) S. Onogi, T. Sato, T. Asada, and Y. Fukui, *J. Polym. Sci., Part A-2*, **8,** 1211 (1970).
(8) H. Kawai, T. Ito, D. A. Keedy, and R. S. Stein, *J. Polym. Sci., Part B*, **2,** 1075 (1964).
(9) T. Ito, T. Oda, H. Kawai, T. Kawaguchi, D. A. Keedy, and R. S. Stein, *Rev. Sci. Instrum.*, **39,** 1847 (1968).
(10) T. Kawaguchi, T. Ito, H. Kawai, D. A. Keedy, and R. S. Stein, *Macromolecules*, **1,** 126 (1968).
(11) A. Tanaka, E. P. Chang, B. Delf, I. Kimura, and R. S. Stein, *J. Polym. Sci., Polym. Phys. Ed.*, **11,** 1891 (1973).
(12) H. Kawai, T. Ito, and S. Suehiro, paper presented at the 18th Annual Symposium on Rheology, Japan, Odawara, Oct. 8, 1969; *Mem. Fac. Eng., Kyoto Univ.*, **32,** 416 (1970).
(13) P. Erhardt and R. S. Stein, *J. Polym. Sci., Part B*, **3,** 553 (1965).
(14) T. Hashimoto, R. E. Prud'homme, D. A. Keedy, and R. S. Stein, *J. Polym. Sci., Polym. Phys. Ed.*, **11,** 693 (1973).
(15) P. Erhardt and R. S. Stein, *J. Appl. Polym. Sci., Appl. Polym. Symp.*, **5,** 113 (1967).
(16) T. Hashimoto, R. E. Prud'homme, and R. S. Stein, *J. Polym. Sci., Polym. Phys. Ed.*, **11,** 709 (1973).
(17) W. T. Chen, *J. Appl. Mech.*, **33,** 539 (1966).
(18) T. T. Wang, *J. Appl. Phys.*, **44,** 4052 (1973).
(19) T. T. Wang, *J. Polym. Sci., Polym. Phys. Ed.*, **12,** 445 (1974).
(20) M. Matsuo, in preparation.
(21) M. Maeda, S. Hibi, F. Itoh, S. Nomura, T. Kawaguchi, and H. Kawai, *J. Polym. Sci., Part A-2*, **8,** 1303 (1970).
(22) S. Suehiro, T. Yamada, H. Inagaki, and H. Kawai, *J. Polym. Sci., Polym. Phys. Ed.*, to be submitted.
(23) J. C. Halpin and J. L. Kardos, *J. Appl. Phys.*, **43,** 2235 (1972).
(24) J. E. Ashton, J. C. Halpin, and P. H. Petit, "Primer on Composite Materials", Technomic, Stamford, Conn. 1968, Chapter 5.
(25) T. T. Wang, *J. Appl. Phys.*, **44,** 2218 (1973).
(26) R. Hill, *J. Mech. Phys. Solids*, **12,** 199 (1964); **13,** 189 (1965).
(27) J. J. Hermans, *Proc. K. Ned. Akad. Wet., Ser. B*, **70,** 1 (1967).
(28) E. Kroner, *Z. Phys.*, **151,** 504 (1958).
(29) S. Nomura, S. Kawabata, H. Kawai, Y. Yamaguchi, A. Fukushima, and H. Takahara, *J. Polym. Sci., Part A-2*, **7,** 325 (1969).
(30) A. Odajima and T. Maeda, *J. Polym. Sci., Part C*, **15,** 55 (1966).
(31) H. D. Keith, M. J. Paddern, Jr., and R. G. Vadimsky, *J. Appl. Phys.*, **42,** 4585 (1971).
(32) S. Hoshino, J. Powers, D. G. LeGrand, H. Kawai, and R. S. Stein, *J. Polym. Sci.*, **58,** 185 (1962).
(33) N. G. McCrum and E. L. Morris, *Proc. R. Soc. London, Ser. A*, **292,** 506 (1966).
(34) H. Kawai, *Rheol. Acta*, **14,** 27 (1975).
(35) S. Clough, J. J. van Aartsen, and R. S. Stein, *J. Appl. Phys.*, **36,** 3072 (1965).
(36) J. J. van Aartsen and R. S. Stein, *J. Polym. Sci., Part A-2*, **9,** 295 (1971).
(37) C. S. M. Ong and R. S. Stein, *J. Polym. Sci., Polym. Phys. Ed.*, **12,** 1899 (1974).
(38) S. Nomura, M. Matsuo, and H. Kawai, *J. Polym. Sci., Polym. Phys. Ed.*, **12,** 1371 (1974).
(39) R. S. Stein and H. B. Rhodes, *J. Appl. Phys.*, **31,** 1873 (1960).
(40) R. J. Samuels, *J. Polym. Sci., Part C*, **13,** 37 (1966).
(41) M. Motegi, T. Oda, M. Moritani, and H. Kawai, *Polym. J.*, **1,** 209 (1970).